

Feature Space Renormalization for Semi-supervised Learning

Jun Sun, Zhongjie Mao, Chao Li, Chao Zhou, Xiao-Jun Wu

Abstract—Semi-supervised learning (SSL) has been proven to be a powerful method for leveraging unlabelled data to alleviate models' dependence on large labelled datasets. The common framework among recent approaches is to train the model on a large amount of unlabelled data with consistency regularization to constrain the model predictions to be invariant to input perturbation. However, the existing SSL frameworks still have room for improvement in the consistency regularization method. Instead of regularizing category predictions in the label space as in existing frameworks, this paper proposes a feature space renormalization (FSR) mechanism for SSL. First, we propose a feature space renormalization mechanism to substitute for the commonly used consistency regularization mechanism to learn better discriminative features. To apply this mechanism, we start by building a basic model and an empirical model and then introduce our mechanism to renormalize the feature learning of the basic model with the guidance of the empirical model. Second, we combine the proposed mechanism with pseudo-labelling to obtain a novel effective SSL model named FreMatch. The experimental results show that our method can achieve better performance on a variety of standard SSL benchmark datasets, and the proposed feature space renormalization mechanism can also enhance the performance of other SSL approaches.

Index Terms—Semi-supervised learning, Feature space renormalization, Feature representation, Pseudo-labelling

1 INTRODUCTION

Deep neural networks (DNNs) have achieved great success in performing computer vision tasks. Such success is partially attributed to the existence of large labelled datasets, for example, ImageNet [1], COCO [2] and other datasets in various fields of computer vision. This means that training DNNs on large labelled datasets can yield better performance with supervised learning [3,4,5]. For many tasks, however, it is challenging to gather extensive accurately labelled data. One reason is that incorrect labels may be added due to subjective factors, and the other is that the cost of labelling can be extremely high since it must be done by professionals manually. For instance, a medical image dataset must be labelled by experienced doctors [6]. In contrast, it is much easier to obtain unlabelled data in most tasks.

A powerful method of training models on a large amount of data without all the labels for the dataset is semi-supervised learning (SSL) [7], which can reduce the demand for labelled data by making the best use of unlabelled data. In many recent SSL approaches, a contrastive loss term is added to the loss function based on unlabelled data to enable the model to generate better predictions for unseen data. There are generally three

choices for this loss term. The first is consistency regularization, which encourages a model to produce the same prediction when the input of the model is randomly modified [8,9,10,11,26]. The second is pseudo-labelling, which employs confident category predictions for unlabelled data as artificial labels to train the model [12,13]. The last method is the holistic method, which aims to integrate the current effective approaches to SSL into a single framework to obtain better performance [14,15].

In this paper, we employ the holistic method to design a new SSL framework, namely, FreMatch, and propose a feature renormalization mechanism based on group representation theory for feature learning to improve the ability to learn a good feature representation of unlabelled data. The difference in learning on unlabelled data between the proposed FreMatch and the recent methods is illustrated in Fig. 1.

Fig. 1 (a) shows the common core framework of the learning process for unlabelled data in recently proposed SSL approaches. Specifically, the input unlabelled image is first preprocessed by different transformation techniques to yield two or more images from different views. Then, the model generates different predictions for these images in the label space. Finally, one of these predictions is regarded as the artificial label, and the other predictions are employed to predict this artificial label. These transformation techniques are either data augmentation methods [10,14,15,16,17] or methods employing adversarial samples [26]. In this work, we apply two different data augmentation methods to transform the input images. They are weak augmentation methods and

- Jun Sun is with the School of Artificial Intelligence and Computer Science and Jiangsu Provincial Engineering Laboratory of Pattern Recognition and Computational Intelligence, Jiangnan University, 1800 Lihu Avenue, Wuxi, Jiangsu 214122. E-mail: junsun@jiangnan.edu.cn; sunjun_wx@hotmail.com
- Zhongjie Mao, Chao Li, Chao Zhou and Xiao-Jun Wu is with the Jiangsu Provincial Engineering Laboratory of Pattern Recognition and Computational Intelligence, Jiangnan University, 1800 Lihu Avenue, Wuxi, Jiangsu 214122.

strong augmentation methods, similar to those used in UDA [14].

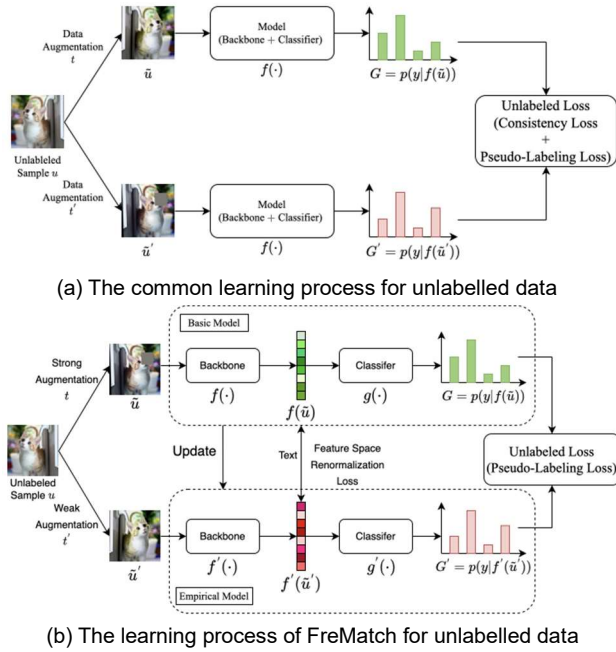


Fig. 1. FreMatch improves the common learning method for unlabelled data from two perspectives. First, without carrying out consistency regularization for comparison after the prediction, we employ feature space renormalization to renormalize the feature representation learned from the unlabelled data. Second, pseudo-labelling is employed to learn the mapping between the feature representation and the corresponding category. Finally, the learning for the unlabelled data is completed by the sequential combination of feature space renormalization and pseudo-labelling.

The framework of the learning process for unlabelled data in the proposed FreMatch is shown in Fig. 1 (b). The two models in FreMatch, called the basic model and the empirical model, have the same structure, and the main difference between them lies in the update strategies for the model weights. Specifically, for the basic model that is learned from the labelled data, we employ back propagation to update the model weights. Additionally, a momentum-based updating approach is adopted to update the empirical model according to the basic model [9]. This method can avoid generating incorrect artificial labels to some extent, which otherwise can inevitably lead the whole training process in an incorrect and uncorrectable direction. The empirical model can also aggregate model weights from the basic model at each training iteration, and it can thus output better intermediate feature representations. Moreover, with the artificial label output by the empirical model, better classification performance can be achieved.

In most recent methods, the loss for unlabelled data is calculated from G and G' , which are predicted class distributions, as shown in Fig. 1(a). These methods focus on either executing sophisticated data perturbation on the unlabelled samples [10, 11, 14, 15] or yielding better pseudo-labels [39]. Different from these methods, in our approach, the learning process for unlabelled data is

divided into two successive steps, as shown in Fig. 1 (b). First, feature space renormalization is performed to renormalize the feature representation learned from the unlabelled data in the feature representation space. Then pseudo-labelling is performed to train the mapping between the feature representation and the data category. Specifically, in FreMatch, strong augmentation and weak augmentation [14,15] are executed simultaneously to generate two different views of the unlabelled data. The artificial label G' is produced for the weakly augmented unlabelled data by the empirical model. The loss term corresponding to feature space renormalization, on the basis of group representation theory, is derived from the condition for isomorphism between the covariance matrix corresponding to the feature representation spaces generated by the empirical model and the basic model. For pseudo-labelling [12], we use only a simple classification layer on the empirical feature representation to generate the artificial classification label, which is utilized only if the model assigns a high probability to one of the possible categories.

FreMatch can obtain better performance on most commonly studied benchmarks for SSL due to our proposed feature space renormalization mechanism and its combination with the pseudo-labelling strategy, which are the main contributions of this paper. In particular, feature space renormalization, as the core of FreMatch, highlights the important role of feature generation and optimization in SSL and reduces the learning pressure on the subsequent classifier. It is an advancement in feature representation learning and is a substitute for consistency regularization, which is widely used in existing SSL methods. As shown in our experimental results, with the help of the feature space renormalization mechanism, our proposed FreMatch achieves generally better or comparable performance on the tested SSL benchmark datasets compared to the other tested methods.

The paper is structured as follows. Section 2 reviews the related work of existing semi-supervised learning methods. In Section 3, the principle and implementation of our proposed FreMatch are described. Section 4 presents the experimental results as well as ablation studies. Finally, the paper is concluded in the last section.

2 RELATED WORKS

In this section, we review some existing methods used in SSL, which are currently state-of-the-art and mainly focus on improvements in consistency regularization and pseudo-labelling methods. Other methods, including transductive learning [18,19], graph-based methods [20,21,22] and generative models [23,24,25,26], are discussed briefly, and one can refer to the survey in [27] for a more comprehensive discussion of these methods.

For a c -class classification task, we define $\mathcal{X} = \{(\mathbf{X}_b, p_b) : b \in (1, \dots, B)\}$ as the batches of labelled feature samples, where \mathbf{X}_b is the b -th batch of labelled feature samples, p_b are the labels corresponding to \mathbf{X}_b , B is the number of sample batches, and b denotes the sample batch number. In addition, we let $\mathcal{U} = \{\mathbf{U}_b : b \in (1, \dots, B)\}$ be

the batches of unlabelled feature samples and denote as $P_{model}(y|x; \theta)$ the prediction distribution for the categories by the model p for input x with parameters θ .

2.1 Consistency Regularization

Consistency has been employed in various loss functions for DNN training. These loss functions, including MSE [28], KL divergence [29, 30] and cross-entropy [31], are used to minimize the gap between the prediction and the label, which means that the prediction and the label should be as consistent as possible. Therefore, consistency is an intrinsic and essential objective in enabling DNNs to learn more effective features. In SSL, consistency regularization is carried out for unlabelled data, relying on the assumption that the model should output the same predictions when fed perturbed views of the same sample. A common perturbation technique is data augmentation [32, 33], which carries out image transformations while keeping the category semantics unaffected. In this work, we also employ data augmentation to add perturbations to unlabelled data. Formally, consistency regularization requires that an unlabelled sample u_i should be classified into the same category as its corresponding augmented sample, i.e., $Augment(u_i)$.

According to the above description, most SSL approaches [14,15] apply the loss term in Equation (1) for a bath of unlabelled data:

$$\frac{1}{n} \sum_{i=1}^n \|P_{model}(y|Augment_1(u_i); \theta) - P_{model}(y|Augment_2(u_i); \theta)\|_2^2 \quad (1)$$

where $Augment_1(\cdot)$ and $Augment_2(\cdot)$ represent two different data augmentation operations, u_i is the i -th sample in the batch, and n is the batch size. For example, in the mean teacher method [9], $Augment_2(\cdot)$ in Equation (1) is defined by the output of the model updated with a moving average approach, and this operation provides a relatively stable feature representation so that it can significantly improve the classification performance. The virtual adversarial training (VAT) method [26] determines an additional perturbation direction, which is applied to the input data, thereby maximizing the change in the distribution of the predicted category. It is essentially a training method with $Augment_2(\cdot)$ in Equation (1) being an adversarial transformation. In MixMatch [10], the MixUp method is used for data augmentation. Based on MixMatch, ReMixMatch was proposed in [11] with two new data augmentation techniques, namely, distribution alignment and augmentation anchoring. In [14], UDA used a weakly augmented sample to generate an artificial label and then enforced the prediction so that the strongly augmented sample was consistent with the artificial label. In UDA, the artificial label is also sharpened to encourage the model to produce predictions with high confidence. FixMatch [15], a simplified version of UDA [14], combines pseudo-labelling and consistency regularization but without the sharpening and training signal annealing in UDA [14]. In SimMatch [34], consistency regularization is carried out at both the semantic level and instance level.

In contrast to consistency regularization, our

proposed feature space renormalization mechanism renormalizes the basic features with the empirical features to make the two feature spaces as homeomorphic as possible, and its output features are the inputs of pseudo-labelling. As will be shown in the subsequent sections, such a mechanism is able to generate generally better feature representations than common consistency regularization.

2.2 Entropy Minimization and Pseudo-labelling

A common assumption in SSL is that the decision boundary of a classifier should not pass through the high-density regions of the marginal data distribution [10]. Entropy minimization [37,38] can satisfy this assumption by encouraging the model to output low-entropy predictions on unlabelled data. This method can be applied explicitly with a loss term that minimizes the entropy of $P_{model}(y|x; \theta)$ for unlabelled data. Another approach that can also satisfy this assumption is pseudo-labelling, which employs the model itself to obtain artificial labels for unlabelled data [35,36]. Moreover, pseudo-labelling can perform entropy minimization implicitly by using ‘‘hard’’ labels when the largest category probability exceeds a predefined threshold [12]. By defining $q_i = P_{model}(y|u_i)$, we can obtain the loss function for unlabelled data as

$$\frac{1}{n} \sum_{i=1}^n \mathbb{1}(\max(q_i) \geq \eta) H(\hat{q}_i, q_i) \quad (2)$$

where $\hat{q}_i = \arg \max(q_i)$, η is a hyperparameter called the threshold, $H(\cdot)$ is the standard cross-entropy loss function, and $\mathbb{1}$ is the mask function. In addition, the $\arg \max$ operation is applied to the output of the model to yield a valid ‘‘one-hot’’ probability distribution. It was shown that the loss in this form, combined with VAT, can lead to good classification performance [26]. Some self-training methods also involve entropy minimization. For instance, in MixMatch [10], a sharpening function is utilized on the target distribution for unlabelled data by implicitly performing entropy minimization. FlexMatch [39] employs curriculum pseudo-labelling (CPL), a curriculum learning approach exploiting unlabelled data according to the learning status of the model. Furthermore, the core of CPL is that it flexibly adjusts the thresholds for different classes at each training iteration, allowing informative unlabelled data and their pseudo-labels to pass the threshold. In FeatMatch [40], a novel learned feature-based refinement and augmentation method is proposed to produce a varied set of good transformations.

In this work, we employ pseudo-labelling not only to produce low-entropy predictions but also to learn a mapping from the feature representation of unlabelled samples to their categories.

2.3 Other Methods Used in Semi-supervised Learning

In addition to the above two kinds of methods commonly used in SSL, researchers have explored various methods in different fields to improve the performance of SSL,

including deep clustering and self-supervised learning. For example, Lerner et al. [41] proposed combining a clustering algorithm with deep SSL methods so that the SSL methods can benefit from real unsupervised learning and are not affected by a small number of possibly uncharacteristic training points. In [42], Wallin et al.

designed a novel consistency regularization approach based on self-supervised learning and combined it with the pseudo-labelling technique so that the model could make full use of all unlabelled data during the training process.

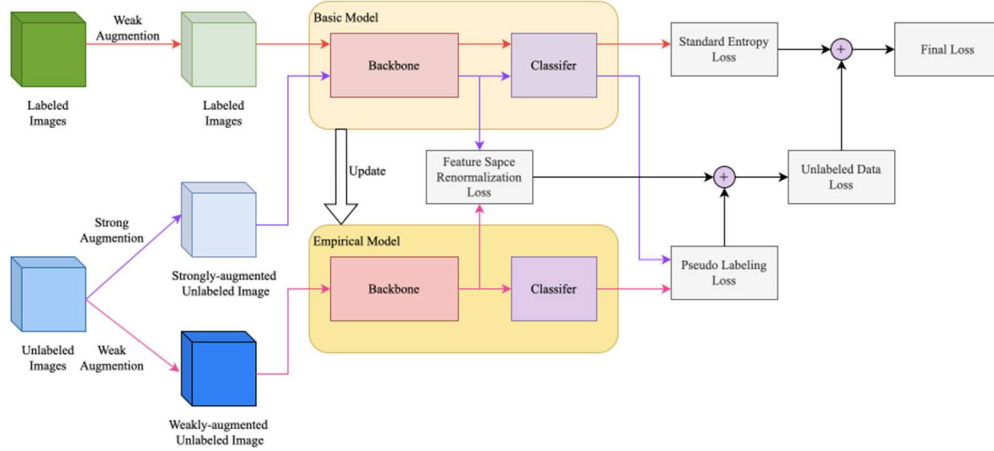


Fig. 2. In the diagram of FreMatch, the red, purple and pink lines represent the processes of the model for labelled data, weakly augmented unlabelled data, and strongly augmented unlabelled data, respectively. For labelled data, we simply compute the standard cross-entropy loss. After making an inference for a batch of labelled samples with the basic model, we immediately update the weights of the empirical model based on the basic model. For unlabelled data, we compute the feature space renormalization loss and the pseudo-labelling loss with the basic model and the empirical model. We obtain the final loss by combining the standard cross-entropy loss and the unlabelled loss.

3 FREMATCH

In this section, we describe in detail the principle and implementation of our proposed FreMatch. First, we present the feature representation based on group representation theory, which is the theoretical foundation of the proposed feature space renormalization mechanism. Second, the principle of feature space renormalization is described. Third, we describe the structure of FreMatch, particularly that of the empirical model in FreMatch. Next, we illustrate how to implement feature space renormalization for FreMatch. Then, the pseudo-labelling method used for FreMatch training is presented. Finally, we provide the total loss function for model training and describe how to train the proposed FreMatch.

In the rest of this section, we still use the notation and definitions in Section 2, and we define two types of augmentations, namely, strong augmentation $\mathcal{A}(\cdot)$ and weak augmentation $a(\cdot)$. For clarity, we show the structure of FreMatch in Fig. 2, which is a refinement of the structure in Fig. 1(b).

3.1 Feature Representation Based on Group Representation Theory

In general, a data sample is represented as a feature vector in a D -dimensional Euclidean space \mathcal{H} , which is called the feature representation space or data space. Mathematically, \mathcal{H} can be regarded as a separable topological space (i.e., Hausdorff space). Therefore, we can represent a set of feature samples as a real $N \times D$ matrix, where N is the sample size and D is the number of features, namely, the dimension of the feature representation space \mathcal{H} . From a

statistical perspective, the general characteristic of the data space is the distribution characteristic of the samples in the space. This characteristic should reflect the symmetry of the space, including translation invariance and rotation invariance. Since the covariance matrix of a given set of samples has a certain invariant characteristic under translation and rotation, it can reflect the symmetry of the data space and therefore represents the fundamental distribution characteristic of the data space.

A covariance matrix is a real $D \times D$ symmetric matrix, and the covariance matrices of all the different feature sample sets in the same feature representation space \mathcal{H} are assembled to compose a subgroup Σ_D of the matrix group GL_D , where GL_D is a general linear group composed of all the $D \times D$ real invertible matrices [43]. We call Σ_D the covariance matrix group of \mathcal{H} . Furthermore, Σ_D is also a topological group since the multiplication and inverse operations on it are essentially continuous maps [43]. Therefore, we can establish the corresponding relation between the Hausdorff space \mathcal{H} and its topological group Σ_D ; that is, Σ_D can represent \mathcal{H} .

For two D -dimensional feature representation spaces \mathcal{H} and \mathcal{H}' , they are said to be topologically the same if they are homeomorphic [44]. Equivalently, a homeomorphism between \mathcal{H} and \mathcal{H}' means that their corresponding covariance matrix groups, Σ_D and $\Sigma_{D'}$, are isomorphic. According to group representation theory, the isomorphism between Σ_D and $\Sigma_{D'}$ requires that for any given sample set S , whose feature sample set represented in \mathcal{H} and \mathcal{H}' are \mathbf{X}_S and \mathbf{X}'_S , respectively, there exists an invertible matrix $\mathbf{P} \in GL_D$ such that

$$\sigma_S = \mathbf{P}^{-1} \sigma'_S \mathbf{P}, \quad (3)$$

where $\boldsymbol{\sigma}_S \in \boldsymbol{\Sigma}_D$ and $\boldsymbol{\sigma}'_S \in \boldsymbol{\Sigma}_{D'}$ are the covariance matrices of \mathbf{X}_S and \mathbf{X}'_S , respectively. Equation (3) essentially means that $\boldsymbol{\sigma}_S$ and $\boldsymbol{\sigma}'_S$ are equivalent matrices. From this equation, we can derive

$$\text{tr}(\boldsymbol{\sigma}_S) = \text{tr}(\mathbf{P}^{-1}\boldsymbol{\sigma}'_S\mathbf{P}) = \text{tr}(\boldsymbol{\sigma}'_S), \quad (4)$$

where $\text{tr}(\cdot)$ denotes the trace of the matrix. In group representation theory [45], $\text{tr}(\cdot)$ is known as the character function for a matrix group, which can characterize the feature representation space to a certain extent.

From the above description, if two feature representation spaces \mathcal{H} and \mathcal{H}' are homeomorphic, or equivalently their corresponding covariance matrix groups $\boldsymbol{\Sigma}_D$ and $\boldsymbol{\Sigma}_{D'}$ are isomorphic, then their character functions are the same. However, the inverse proposition does not hold; that is, we cannot derive Equation (3) from Equation (4) since $\text{tr}(\cdot)$ is a group homomorphism but not necessarily a bijection [45].

3.2 Feature Space Renormalization

According to the above analysis, we introduce our proposed feature space renormalization mechanism as follows.

Feature space renormalization is carried out on the features to make the two feature representation spaces \mathcal{H} and \mathcal{H}' homeomorphic, or equivalently to make their corresponding covariance matrix groups $\boldsymbol{\Sigma}_D$ and $\boldsymbol{\Sigma}_{D'}$ isomorphic. Without loss of generality, we denote \mathbf{X}_S and \mathbf{X}'_S as the centralized feature sample sets for the data sample set S in the feature representation spaces \mathcal{H} and \mathcal{H}' , respectively. Here, centralization means that each dimension of each sample vector is decreased by the average value of the corresponding dimension. Therefore, the covariance matrices for \mathbf{X}_S and \mathbf{X}'_S are given by

$$\boldsymbol{\sigma}_S = \mathbf{X}_S^T \mathbf{X}_S \quad (5)$$

and

$$\boldsymbol{\sigma}'_S = \mathbf{X}'_S{}^T \mathbf{X}'_S. \quad (6)$$

To make $\boldsymbol{\Sigma}_D$ and $\boldsymbol{\Sigma}_{D'}$ isomorphic or $\boldsymbol{\sigma}_S$ and $\boldsymbol{\sigma}'_S$ equivalent, we could use Equation (4) as the constraint condition, that is, minimize $|\text{tr}(\boldsymbol{\sigma}_S) - \text{tr}(\boldsymbol{\sigma}'_S)|$ during feature learning. However, as addressed above, Equation (4) cannot guarantee the equivalence between $\boldsymbol{\sigma}_S$ and $\boldsymbol{\sigma}'_S$, and moreover, it can lead to information loss during feature learning if only equivalence between the character functions is required. Hence, we have to employ Equation (3) to make $\boldsymbol{\sigma}_S$ and $\boldsymbol{\sigma}'_S$ equivalent. To this end, we assume there exists a mapping $\mathcal{C}: \mathcal{H}' \rightarrow \mathcal{H}$ such that

$$\mathbf{X}_S^T = \mathcal{C} \mathbf{X}'_S{}^T \quad (7)$$

where \mathcal{C} is a $D \times D$ real matrix. Consequently, from Equations (5) and (7), we can obtain

$$\boldsymbol{\sigma}_S = \mathbf{X}_S^T \mathbf{X}_S = \mathcal{C} \mathbf{X}'_S{}^T \mathbf{X}'_S \mathcal{C}^T. \quad (8)$$

By substituting (6) into (8), we have

$$\boldsymbol{\sigma}_S = \mathcal{C} \boldsymbol{\sigma}'_S \mathcal{C}^T. \quad (9)$$

Comparing Equation (9) with Equation (3), we find that if $\mathcal{C}^T = \mathbf{P}$ and $\mathcal{C} = \mathbf{P}^{-1}$, or equivalently, if

$$\mathcal{C}^T \mathcal{C} = \mathbf{I}_D, \quad (10)$$

then $\boldsymbol{\sigma}'_S$ is equivalent to $\boldsymbol{\sigma}_S$ so that the two feature representation spaces are homeomorphic or the same. Here, \mathbf{I}_D is the $D \times D$ identity matrix, and Equation (10) indicates that \mathcal{C} should be an orthogonal matrix to satisfy Equation (3). Therefore, Equations (7) and (10) together can be employed as the constraints during the training process, and all the elements of \mathcal{C} can be learnable parameters. Such a mechanism using Equations (7) and (10) as the constraint to ensure the consistency of the two models at the feature level is called feature space renormalization. In the rest of this section, we will further describe how to implement feature space renormalization for our proposed FreMatch.

3.3 Empirical Model

Generally, a DNN model is employed to generate the feature representation for the given samples. In this paper, we use the basic model in FreMatch for this purpose, with the help of an empirical model.

Specifically, we need to learn semantic information from both labelled data and unlabelled data. First, before the training process, the basic model and the empirical model are exactly the same; that is, the two models have the same structure and initialized weights. Then, during the training process, the basic model makes an inference for a batch of labelled data and obtains a classification loss, and afterwards, the empirical model updates its weights according to the following formula:

$$\theta'_t = m\theta'_{t-1} + (1-m)\theta_t, \quad (11)$$

where θ'_t is the set of weights of the empirical model at training iteration t , θ_t is the set of weights of the basic model at training iteration t , and $m \in [0, 1)$ is a momentum coefficient. Next, a batch of unlabelled data is input to the basic model and the empirical model simultaneously to obtain the feature space renormalization loss and the pseudo-labelling loss, which will be described in the next subsections. Combining the above classification loss for labelled data with these two losses, we can update the weights of the basic model by carrying out back propagation.

The empirical model can aggregate useful semantic information for classification from the basic model after each training iteration. In addition, since the momentum weights improve the outputs of all the layers, not just the last layer, the empirical model has a better intermediate representation for unlabelled data than the basic model. This is very suitable for the implementation of our proposed feature space renormalization mechanism. As shown in Fig. 1 (b), we divide the basic model into two parts, namely, $f(\cdot)$ and $g(\cdot)$, and we divide the empirical model into $f'(\cdot)$ and $g'(\cdot)$. Here, $f(\cdot)$ and $f'(\cdot)$ are used as the feature extraction model, and feature space renormalization is performed on their output features. Specifically, for an unlabelled sample u , after strong augmentation and weak augmentation, the resultant samples are \tilde{u} and \tilde{u}' , which are input to $f(\cdot)$ and $f'(\cdot)$. The output feature samples $f(\tilde{u})$ and $f'(\tilde{u}')$ of $f(\cdot)$ and

$f'(\cdot)$ are then employed to carry out feature space renormalization. After that, $g(\cdot)$ and $g'(\cdot)$ are used as the classification layer to implement pseudo-labelling. More details of the above procedure in Fig. 1(b) are shown in Fig. 2 and described in the next subsections.

3.4 Implementation of FSR for FreMatch

In this subsection, we will illustrate in detail how to implement the feature space renormalization mechanism for FreMatch and then deduce its loss function.

Since DNN models are generally trained with the stochastic gradient descent (SGD) method based on each randomly selected batch of training samples, feature space renormalization is carried out on each batch of unlabelled samples during the training process. For the b -th batch of unlabelled samples, as shown in Fig. 1(b) and Fig. 2, strong augmentation and weak augmentation are carried out on the unlabelled sample batch, and the resultant sample batches are fed to the basic model and the empirical model, respectively, for model training. After feature extraction with $f(\cdot)$ and $f'(\cdot)$, the feature representation spaces for the basic model and the empirical model are transformed into be \mathcal{H} and \mathcal{H}' , respectively, and the corresponding augmented sample batches are mapped into \mathcal{H} and \mathcal{H}' and represented as $\mathbf{U}_b \in \mathbb{R}^{n \times d}$ and $\mathbf{U}'_b \in \mathbb{R}^{n \times d}$, respectively. Here, \mathbf{U}_b and \mathbf{U}'_b are centralized, n is the size of the unlabelled sample batch, and d is the dimension of the output feature vectors of $f(\cdot)$ and $f'(\cdot)$, namely, the dimension of \mathcal{H} and \mathcal{H}' .

Following the feature space renormalization mechanism proposed in subsection 3.2, we assume that there exists a mapping $\mathcal{C}: \mathcal{H}' \rightarrow \mathcal{H}$ such that

$$\mathbf{U}'_b = \mathcal{C}\mathbf{U}_b^T, \quad (12)$$

as in Equation (7). Thus, the condition for an isomorphism existing between the covariance matrices of \mathcal{H} and \mathcal{H}' is

$$\mathcal{C}^T \mathcal{C} = \mathbf{I}_d, \quad (13)$$

which is identical to Equation (10) except that the dimension of the feature representation spaces is d .

However, it should be emphasized here that although the network structures of $f(\cdot)$ and $f'(\cdot)$ are the same, there is some difference between the weakly augmented sample batch fed to $f(\cdot)$ and the strongly augmented sample batch fed to $f'(\cdot)$. In this sense, the unlabelled sample batches input to the empirical model and the basic model cannot be considered to be completely identical for feature extraction, so the condition for feature space renormalization in Equation (13) is too strict, and it is reasonable to use a weaker condition to replace it.

A feasible scheme of weakening the condition in Equation (13) is to not require the orthogonality of \mathcal{C}^T or \mathcal{C} . As a result, the right side of Equation (13) should not be the identity matrix. Considering that $\mathcal{C}^T \mathcal{C}$ is a real symmetric matrix and the number of parameters to be learned during the training process should be as small as possible, we change Equation (13) to

$$\mathcal{C}^T \mathcal{C} = \mathbf{I}_d \text{diag}(\varepsilon_1 \varepsilon_2, \dots, \varepsilon_d) \quad (14)$$

$$= \text{diag}(\varepsilon_1, \varepsilon_2, \dots, \varepsilon_d) = \begin{pmatrix} \varepsilon_1 & & \\ & \ddots & \\ & & \varepsilon_d \end{pmatrix},$$

where $\text{diag}(\varepsilon_1, \varepsilon_2, \dots, \varepsilon_d)$ is a diagonal matrix and $0 \leq \varepsilon_j \leq 1$ ($1 \leq j \leq d$) is called the tolerance in the j -th dimension.

Hence, we obtain the feature space renormalization conditions for FreMatch as Equations (12) and (14) and rewrite them together as

$$\begin{aligned} \mathbf{U}'_b &= \mathcal{C}\mathbf{U}_b^T, \\ \mathcal{C}^T \mathcal{C} &= \text{diag}(\varepsilon_1, \varepsilon_2, \dots, \varepsilon_d), \end{aligned} \quad (15)$$

which is thus employed as the constraint for feature space renormalization during the training process. Here, \mathcal{C} and ε_j ($1 \leq j \leq d$) are the parameters to be learned during the model training.

3.5 Pseudo-labelling

Following the above procedure, the feature representations output by $f'(\cdot)$ and $f(\cdot)$ are further used for pseudo-labelling by implementing $g(\cdot)$ and $g'(\cdot)$, respectively. Classifiers $g(\cdot)$ and $g'(\cdot)$, both of which are maps from $\mathbb{R}^{n \times d}$ to $\mathbb{R}^{n \times c}$, are used to determine the prediction distribution. Here, c denotes the number of categories. However, the classification blocks are only able to learn category information from labelled data. Therefore, we perform pseudo-labelling to train the discrimination ability of the basic model for unlabelled data.

For unlabelled data, we obtain artificial labels from the empirical model and use these labels to compute the standard cross-entropy with the predictions obtained from the basic model. Specifically, we obtain the prediction distribution of categories $q_i = P_{\text{empirical}}(y|a(u_i))$ by applying the empirical model to the weakly augmented unlabelled samples and then obtain $\hat{q}_i = \arg \max(q_i)$. To learn better discrimination, we employ \hat{q}_i as the artificial label when it is higher than a specified confidence threshold. Finally, we can obtain the loss function for pseudo-labelling ℓ_{pl} as

$$\ell_{pl} = \frac{1}{n} \sum_{i=1}^n \mathbb{1}(\max(q_i) > \eta) H(\hat{q}_i, p_{\text{base}}(y|\mathcal{A}(u_i))), \quad (16)$$

where η is a scalar hyper-parameter denoting the confidence threshold.

3.6 The Loss Function for FreMatch

The network structure of FreMatch is illustrated in Fig. 2, and the final loss function for training the network is

$$\mathcal{L} = \ell_{sup} + \lambda \ell_{usp}, \quad (17)$$

where ℓ_{sup} is the supervised cross-entropy loss for weakly augmented labelled data, ℓ_{usp} is the unsupervised loss for unlabelled data, and λ is a fixed scalar hyperparameter representing the relative weight of ℓ_{usp} . Here, ℓ_{sup} is defined by:

$$\ell_{sup} = \frac{1}{n} \sum_{i=1}^n H(p_i, P_{basic}(a(x_i))). \quad (18)$$

The unsupervised loss function includes the loss for pseudo-labelling in Equation (16). Thus, the training of models aims to minimize the loss function in Equation (17) subject to the feature space renormalization constraints in Equation (15). There are $d^2 + d$ equality constraints in Equation (15), and these constraints can be converted to the following penalty function:

$$\ell_{fre} = l_m(\mathbf{U}_b^T - \mathbf{C}\mathbf{U}_b^T) + \beta l_m(\mathbf{C}^T \mathbf{C} - \text{diag}(\varepsilon_1, \varepsilon_2, \dots, \varepsilon_d)), \quad (19)$$

where β is a scalar hyperparameter, $l_m(\cdot)$ denotes the mean of the squares of all the equality constraints, and ℓ_{fre} is also called the loss term for feature space renormalization. Since feature space renormalization is implemented for unlabelled samples, we take the sum of ℓ_{fre} and ℓ_{pl} as the unsupervised loss ℓ_{usp} ; that is,

$$\ell_{usp} = \ell_{fre} + \ell_{pl}, \quad (20)$$

where ℓ_{fre} is used to learn more discriminative feature representations, and ℓ_{pl} , the loss term for pseudo-labelling in (16), is employed to learn the mapping from the feature representation to the artificial label. It should be noted that λ also essentially plays the role of the penalty coefficient for ℓ_{fre} , which is also one of the reasons why λ should take a large value during model training.

3.7 Training of FreMatch

Model learning in SSL should generally focus on labelled data (i.e., supervised learning) during the early stage of the training process since learning on labelled data can lay a solid foundation for learning on unlabelled data. After sufficient learning on labelled data, the focus of the training process should shift to learning on unlabelled data. For SSL methods, such a learning process requires gradually adjusting the weights of the two loss terms.

A commonly used method is to gradually increase λ in Equation (17) but not to employ the threshold η in pseudo-labelling. The reason is as follows. ℓ_{usp} is relatively large at the beginning of training. However, as we explained above, learning on labelled data is more important at this time. Thus, λ should be set to a small value to suppress ℓ_{usp} . As the training progresses, when ℓ_{sup} decreases to a small enough value, the learning on labelled data is sufficient, and learning on unlabelled data becomes more important from this time on. The increasing λ can thus achieve such a shift between the importance of ℓ_{sup} and the importance ℓ_{usp} for model training.

In our method, we fix the value of λ during the training process and set the threshold η for pseudo-labelling to achieve the above goals. At the beginning of training, since the empirical model cannot give predictions with high confidence, the $\max(q_b)$ values of most unlabelled data are smaller than the threshold, and the loss

of this part of the data is not calculated in the final loss function. As such, the loss of unlabelled data, ℓ_{usp} , is very small at the beginning, so the focus of FreMatch training is on labelled data. As the training progresses, the empirical model can gradually produce high-confidence predictions. At the same time, ℓ_{usp} becomes larger than ℓ_{sup} , and thus, the focus of model learning gradually shifts to learning on unlabelled data. To ensure that this occurs, we can fix λ at a large value during the training process, which also essentially gives great penalties to ℓ_{fre} .

4 EXPERIMENTS

We evaluated the performance of FreMatch on several standard SSL datasets, including CIFAR-10 [46], CIFAR-100 [46], SVHN [47], and STL10 [50], as well as on ImageNet [1], and some other object recognition datasets. Some models with state-of-the-art performance were used as baselines for performance comparison. Moreover, different numbers of labelled samples were used in the experiments on these datasets for the purpose of comprehensive performance evaluation. The experimental results involves the performance comparison on the tested datasets, the comparison of training costs, and the results for the ablation study.

FreMatch employed a weak augmentation method that solely consists of flip-and-shift transformations. Specifically, the images were flipped horizontally with a probability of 0.5 followed by a random translation with a maximum distance of 0.125 of the image height. The strong augmentation used in FreMatch was RandAugment [51] followed by Cutout [16].

In all the experiments carried out in this work, the training of FreMatch was carried out for 400 epochs for each dataset, by using the SGD method based on each randomly selected batch of training samples.

4.1 Results for the Benchmark Datasets

4.1.1 Experimental Settings

In the experiments on the benchmark datasets (i.e. CIFAR-10, CIFAR-100, SVHN, and STL-10), we trained the model by using the SGD with a momentum of 0.9 and a weight decay of 1e-3 but without the Nesterov variant of momentum. The initial learning rate was set to 0.01, and the cosine scheduler was used for the gradual decay of the learning rate.

For performance comparison, we implemented all the baseline models in the same codebase and employed the Wider ResNet network [52] as the backbone network for the purpose of fair comparison as recommended in [48]. In detail, Wider ResNet-28-2 was employed for the CIFAR-10 and SVHN datasets, Wider ResNet-28-8 for CIFAR-100, and Wider ResNet-37-2 for STL-10. The entire training protocol, including the optimizer, learning rate schedule and data preprocessing, was the same for the same dataset. The baseline models we chose for performance comparison included Π -Model [49], Mean Teacher [9], Pseudo-Label [12], MixMatch [10], ReMixMatch [11], UDA

[14], FixMatch [15], FlexMatch [39], DoubleMatch [42], FeatMatch [40], Meta pseudo-labelling [53], SimMatch [34], NP-Match [54] and Semi-Clustering [41]. Among them, the Π -Model, Mean Teacher, and Pseudo-Label are classical methods for SSL. In essence, MixMatch, ReMixMatch and UDA were obtained by exploiting the influence of different data augmentation methods used in SSL. Fixmatch employs both pseudo-labelling and consistency regularization methods for its loss function. In DoubleMatch and FeatMatch, the consistency regularization method is improved based on FixMatch, while in FlexMatch, the pseudo-labelling method is enhanced based on FixMatch. Meta pseudo-labelling, SimMatch, NP-Match, and Semi-Clustering employ new

training strategies or integrate self-supervised learning and deep clustering methods under the framework of FixMatch. The hyper-parameter settings for all the other compared methods were set according to the settings in their corresponding papers.

Since the works proposing some of the compared models did not involve performance tests on some of the benchmark datasets used in this work, we performed experiments with these models on these datasets and compared the results with those of our proposed FreMatch. The mean and standard deviation (STD) of the error rates obtained by each model were also determined after the model was trained three times on different numbers of labelled samples for each dataset.

TABLE 1
The Error Rates for CIFAR-10 with Five Different Numbers of Labelled Images

Model	CIFAR-10				
	250 labels	500 labels	1000 labels	2000 labels	4000 labels
Π -Model [49]	54.26±3.97	41.82±1.52	31.53±0.98	23.07±0.66	14.01±0.38
Mean Teacher [9]	47.32±4.71	42.01±5.86	17.32±4.00	12.17±0.22	9.19±0.19
Pseudo-Label [12]	49.98±1.17	40.55±1.70	30.91±1.73	21.96±0.42	16.21±0.11
MixMatch [10]	11.08±0.87	9.65±0.94	7.75±0.32	7.03±0.15	6.24±0.06
ReMixMatch [11]	6.27±0.34	6.04±0.04	5.73±0.16	5.53±0.18	5.14±0.04
UDA [14]	5.43±0.96	4.80±0.09	4.75±0.10	4.73±0.14	4.32±0.08
FixMatch [15]	5.07±0.65	4.85±0.06	4.73±0.34	4.54±0.12	4.26±0.05
FlexMatch [39]	4.98±0.49	4.47±0.34	4.22±0.05	4.18±0.12	4.19±0.01
Semi-Clustering [41]	5.51±0.25	5.40±0.23	4.88±0.14	4.71±0.12	4.62±0.09
DoubleMatch [42]	5.56±0.42	5.12±0.43	4.99±0.05	4.66±0.23	4.65±0.17
FeatMatch [40]	7.50±0.64	6.21±0.11	5.76±0.07	4.95±0.20	4.91±0.18
MPL [43]	5.76±0.26	5.89±0.23	5.72±0.15	4.40±0.04	3.89±0.07
SimMatch [34]	4.84±0.13	4.62±0.21	4.34±0.04	4.12±0.14	3.96±0.01
NP-Match [54]	4.96±0.04	4.90±0.11	4.84±0.12	4.32±0.05	4.11±0.02
FreMatch (ours)	4.95±0.34	4.62±0.22	4.24±0.13	3.90±0.14	3.47±0.11

TABLE 2
The Error Rates for SVHN with Five Different Numbers of Labelled Images

Model	SVHN				
	250 labels	500 labels	1000 labels	2000 labels	4000 labels
Π -Model [49]	18.96±1.92	11.44±0.39	8.60±0.18	6.94±0.27	5.57±0.14
Mean Teacher [9]	6.45±2.43	3.82±0.17	3.75±0.10	3.51±0.09	3.39±0.11
Pseudo-Label [12]	21.16±0.88	14.35±0.37	10.19±0.41	7.54±0.27	5.71±0.07
MixMatch [10]	3.78±0.26	3.64±0.46	3.27±0.31	3.04±0.13	2.89±0.06
ReMixMatch [11]	3.10±0.50	3.02±0.33	2.83±0.30	2.63±0.02	2.42±0.09
UDA [14]	2.74±2.76	2.55±0.09	2.35±0.07	2.20±0.06	2.28±0.10
FixMatch [15]	2.48±0.38	2.35±0.05	2.28±0.11	2.25±0.10	2.20±0.09
FlexMatch [39]	6.59±2.29	6.79±1.20	6.72±0.30	4.88±0.23	4.45±0.12
Semi-Clustering [41]	2.30±0.03	2.29±0.03	2.26±0.12	2.21±0.04	2.15±0.12
DoubleMatch [42]	2.41±0.53	2.50±0.23	2.25±0.09	2.20±0.13	2.15±0.09
FeatMatch [40]	3.34±0.19	3.08±0.12	3.10±0.06	2.77±0.33	2.62±0.08
MPL [53]	2.29±0.03	2.30±0.12	2.28±0.07	2.30±0.03	2.18±0.12
SimMatch [34]	6.61±0.21	6.45±0.20	6.11±0.04	3.01±0.11	2.97±0.07
NP-Match [54]	3.92±0.15	2.55±0.12	2.47±0.23	2.27±0.01	2.28±0.04
FreMatch (ours)	2.34±0.32	2.28±0.12	2.20±0.13	2.21±0.06	2.14±0.03

4.1.2 Experimental Results for CIFAR-10, CIFAR-100 and SVHN

In this subsection, we make performance comparisons

between FreMatch and other SSL methods on the CIFAR-10, CIFAR-100 and SVHN benchmarks. The training set and testing set in CIFAR-10 (including 10 categories) contain 50,000 images and 10,000 images, respectively.

CIFAR-100 has 100 categories of images, 50,000 in the training set and 10,000 in the testing set. SVHN also contains 10 categories of images, 73,257 in the training set and 26,032 in the testing set.

During the training process, the hyper-parameters were set as $\lambda = 20.0$, $\eta = 0.95$, $m = 0.9$ and $\beta = 1.0$ for CIFAR-10 and SVHN and as $\lambda = 25.0$, $\eta = 0.95$, $m = 0.97$ and $\beta = 1.0$ for CIFAR-100. For CIFAR-10 and SVHN, the parameter d , i.e., the dimension of the feature space, was set to 128, and for CIFAR-100, it was set to 256.

We show the results of all the baselines and FreMatch on each dataset in Tables 1 to 3. We do not present here the results with 40 labels per class for Π -Model, Mean Teacher and Pseudo-Label since their performance was poor on CIFAR-100. FixMatch, FlexMatch and SimMatch all

performed well on different numbers of labelled samples selected from the benchmark dataset. However, the proposed FreMatch can achieve performance that is better than or comparable to that of the other compared methods in all of the cases.

Table 1 shows the results obtained by all the compared methods for CIFAR-10. FreMatch obtained the lowest error rate in the experiments with 200 and 400 labels per class. However, some state-of-the-art methods had better performance than FreMatch on the other numbers of labelled samples. For example, when only 250 labels were available, the error rate of FreMatch was higher than that of SimMatch by 0.11%; when 500 labels were used, the error rate of FreMatch was higher than that of FlexMatch by 0.15%.

TABLE 3
The Error Rates for CIFAR-100 with Four Different Numbers of Labelled Images

Model	CIFAR-100			
	400 labels	1000 labels	2500 labels	10000 labels
Π -Model [49]	-	66.75±0.34	57.38±0.46	37.88±0.11
Mean Teacher [9]	-	60.99±0.21	53.91±0.57	36.21±0.19
Pseudo-Label [12]	-	62.78±0.33	57.38±0.46	36.21±0.19
MixMatch [10]	67.61±1.32	54.73±0.24	39.94±0.37	28.31±0.33
ReMixMatch [11]	44.28±2.06	37.86±0.55	27.43±0.31	23.03±0.56
UDA [14]	59.28±0.88	45.20±0.71	33.13±0.22	24.50±0.25
FixMatch [15]	48.85±1.75	40.55±0.09	28.29±0.11	23.03±0.56
FlexMatch [39]	39.94±1.62	38.44±1.20	26.49±0.20	21.90±0.15
Semi-Clustering [41]	66.57±0.23	54.01±0.12	44.35±0.03	35.99±0.23
DoubleMatch [42]	42.61±1.15	42.05±0.34	27.47±0.19	21.69±0.26
FeatMatch [40]	48.70±0.42	41.85±0.23	30.43±0.04	26.83±0.04
MPL [49]	44.49±0.99	38.13±0.23	27.43±0.22	22.79±0.18
SimMatch [34]	39.29±1.51	37.12±0.52	25.21±0.32	20.63±0.11
NP-Match [54]	38.91±0.99	37.43±0.55	26.06±0.26	21.22±0.13
FreMatch (ours)	47.15±1.32	37.22±0.24	26.13±0.23	21.25±0.11

As shown in Table 2, FreMatch consistently performed well on SVHN for most of the different numbers of labelled samples, with the lowest error rates among all the models for 500 to 4000 labels. For example, the classification accuracy of FreMatch was 4.27% higher than that of SimMatch when 250 labelled samples were used. Moreover, by utilizing 500 and 1000 labelled samples, the classification errors of FreMatch were 4.51% and 4.52% lower than those of FlexMatch, respectively. However, in the case of a small number of labelled samples (i.e., 250 labelled samples), the error rate of FreMatch was higher than that of Semi-Clustering by 0.04%.

The performance comparison among the tested approaches for CIFAR-100 is illustrated in Table 3. The proposed FreMatch achieved competitive results when different numbers of labelled samples were used. It performed worse than SimMatch, with an error rate only 0.1% higher than that of SimMatch, when employing 1000 labelled samples. However, when a very small number of labelled samples were used (e.g., 4 labels per class and 400 in total), SimMatch obtained a lower error rate than FreMatch by nearly 12%. The reason why FreMatch did not perform better than its competitors in the case of a very small number of labels will be addressed in subsection 4.2.

Additionally, according to the results in Tables 1 to 3, using a small number of labelled samples introduces greater randomness in training, so the variances of the error rates of FreMatch are relatively large. In addition, the random data augmentation method may lead to larger variances.

4.1.3 Experimental Results for STL-10

STL-10 is a dataset specifically designed for the performance evaluation of SSL methods, with 5,000 labelled images and 100,000 unlabelled images. It is inspired by the CIFAR-10 dataset with some modifications. In particular, each category in STL-10 has fewer labelled training samples than in CIFAR-10, but the STL-10 dataset provides a large number of unlabelled samples. The difference in the distributions between the labelled images and the unlabelled images makes the testing tasks on this dataset more challenging and closer to real application scenarios. During the training process, we set the hyperparameters as $\lambda = 20.0$, $\eta = 0.95$, $m = 0.9$ and $\beta = 1.0$. The parameter d , i.e., the dimension of the feature space, was set to 128. As shown in Table 4, FreMatch achieved very competitive performance. When 1000 labelled samples were used, the error rate of FreMatch was

lower than that of NP-Match by 0.57%. However, NP-Match achieved the best accuracy with 4 labels per class, i.e., 40 labels in total.

TABLE 4
The Error Rates for STL10 on Two Different Numbers of Labelled Images

Model	STL10	
	40 labels	1000 labels
Π -Model [49]	-	26.23±0.82
Mean Teacher [9]	-	21.43±2.39
Pseudo-Label [12]	74.76±0.99	27.99±0.80
MixMatch [10]	54.93±0.96	10.41±0.61
ReMixMatch [11]	32.12±6.24	5.23±0.45
UDA [14]	37.42±8.44	7.66±0.56
FixMatch [15]	35.97±4.14	5.17±0.63
FlexMatch [39]	29.15±4.16	5.77±0.23
Semi-Clustering [41]	40.90±0.23	4.78±0.29
DoubleMatch [42]	34.34±0.34	4.46±0.20
FeatMatch [40]	51.26±0.33	6.94±0.32
MPL [53]	35.76±3.29	6.45±0.29
SimMatch [34]	37.57±0.23	5.63±0.35
NP-Match [54]	14.20±0.67	5.59±0.24
FreMatch (ours)	36.12±0.77	5.02±0.22

4.2 Results For Other Object Recognition Datasets

We also tested the proposed method on some new object recognition datasets. Although these datasets are domain adaptation datasets, they can also be employed to evaluate semi-supervised frameworks.

Office31 [55] contains 4110 images in 31 categories, and each category is from 3 domains, i.e., Amazon, Webcam, and Dslr. The Office-Home dataset [56] consists of images from 4 different domains, namely, Artistic images, Clip Art, Product images and Real-World images. For each domain, the dataset contains images in 65 object categories typically found in office and home settings. The latest version of the dataset contains approximately 15,500 images in the 65

categories. The DomainNet dataset [57] is the largest domain adaptation dataset to date, and it contains six domains, with each domain containing 345 categories of common objects.

We first divided each of these datasets into training and testing sets. The domain adaptation datasets contain different numbers of images per category, and the different domains of each category also contain different numbers of images. Therefore, we took 70% of the images in each domain of each category as training samples and the remaining 30% as testing samples. The training set and testing set in Office31 contain 3,253 images and 857 images, respectively. Office-home has 15,588 images, with 10,588 in the training set and 5,000 in the testing set. DomainNet includes 586,575 images, 409,832 in the training set and 176,743 in the testing set.

We tested the proposed FreMatch as well as FlexMatch, ReMixMatch, FixMatch, DoubleMatch, SimMatch and NP-Match on the datasets and made performance comparisons among them since they can achieve better performance on commonly used SSL datasets. The results of fully supervised experiments for each dataset are also provided for a better understanding of the performance of SSL algorithms. The fully-supervised experiments were conducted with all the labelled training samples, and weak augmentation was employed. Therefore, the loss function for the fully-supervised experiments, denoted as ℓ_{full} , is given by

$$\ell_{full} = \frac{1}{n} \sum_{i=1}^n H(y_i, P_m(a(x_i))), \quad (17)$$

where x_i is the i -th sample in a batch of labelled data, y_i is its label, n is the batch size, and the other notations in the equation is explained in the previous sections. For the domain adaptation datasets, each category contains multiple domains, and there are significant differences among these domains, which makes it difficult for fully-supervised training to achieve very good performance. Generally, domain adaptation datasets are more complex and challenging than the datasets commonly used for semi-supervised frameworks.

TABLE 5
The Error Rates for Other Object Recognition Datasets with Different Numbers of Labelled Images.
(The numbers of data categories contained in each domain adaptation dataset are given.)

Model	Office31(31)	Office-home (65)		DomainNet (345)	
	10 labels per class	10 labels per class	50 labels per class	50 labels per class	500 labels per class
ReMixMatch [11]	30.12±0.33	68.69±0.07	46.42±0.36	82.54±0.11	76.23±0.23
FixMatch [15]	28.36±0.20	55.73±0.23	46.27±0.23	79.12±0.03	73.79±0.15
FlexMatch [39]	25.13±0.33	54.56±0.30	43.99±0.03	66.12±0.15	53.45±0.23
DoubleMatch [42]	26.30±0.30	56.45±0.13	45.25±0.13	70.32±0.32	55.43±0.12
SimMatch [34]	26.09±0.12	53.65±0.09	45.01±0.04	65.95±0.20	51.33±0.04
NP-Match [54]	25.05±0.20	55.01±0.43	44.03±0.12	66.44±0.18	51.40±0.08
FreMatch	25.01±0.46	55.43±0.36	43.42±0.19	65.89±0.23	50.53±0.07
Fully-Supervised	13.54±0.10	32.48±0.03		43.37±0.23	

For a fair comparison, we used the same hyperparameters in the experiments for the different compared methods. Specifically, the optimizer used in all the experiments was SGD with a momentum of 0.9 and a weight decay of 10^{-3} but without the Nesterov variant of momentum. The initial learning rate was set to 0.01, and the cosine scheduler was used for the gradual decay of the learning rate. We set λ , the weight of the unlabelled loss, to 1.0 for FixMatch, FlexMatch, SimMatch and NP-Match; 1.5 for ReMixMatch; and 20.0 for FreMatch. These settings of λ followed those recommended in the corresponding original literature. We also employed the wider ResNet-28 network as the backbone network for the fully supervised experiments and SSL experiments. Additionally, we computed the mean and standard deviation (STD) of the classification error rates after three model training iterations on different numbers of labelled samples. As shown in Table 5, on the most complex dataset, i.e., DomainNet, the error rate of the fully supervised classification model was 43.37%. All the SSL models had a relatively obvious performance gap with respect to the fully supervised methods on the domain adaptation datasets. FreMatch achieved better classification performance in most of the experiments. However, similar to the results for the above tested datasets, such as CIFAR-100 and STL-10, when only a very small number of labelled samples were provided for each category, the performance of FreMatch was slightly inferior to those of some other methods.

4.3 Results For ImageNet-1k

To further evaluate the performance of our proposed method, we also tested FreMatch and other methods (i.e., FixMatch, FlexMatch, and NP-Match) on the large-scale ImageNet-1k dataset [1]. Specifically, for ImageNet, we employed 10% of the samples of the whole training set as labelled data, approximately 128,000 images, and the rest of the data were used as unlabelled data. The testing set for the SSL methods compared in this set of experiments was the standard ImageNet testing dataset, which has 50,000 samples. Furthermore, the image resolution for ImageNet was set as 128×128 .

TABLE 6

The Top-1 Error Rate and Top-5 Error Rate of Each Method on ImageNet with 10% Labelled Images

Method	Top-1	Top-5
FixMatch [15]	43.16	21.80
FlexMatch [39]	41.83	19.20
NP-Match [50]	41.78	19.33
FreMatch	41.80	19.20

For ImageNet, the ResNet-50 [58] model was used as the backbone network, which is also commonly employed by previous works in SSL. During the training process, the hyperparameters were set as $\lambda = 25.0$, $\eta = 0.85$, and $\beta = 0.1$. We employed SGD with an initial learning rate of 0.03,

momentum of 0.9 and weight decay of $3e-4$. Additionally, the cosine scheduler was adopted for the gradually decaying learning rate, and the batch size n was set to 64. For the training process, similar to the previous datasets, we needed to train the basic and empirical models. However, for training the empirical model, we employed a flexible method of updating the weights, which allowed us to obtain a more stable empirical model for large-scale datasets. Here, the momentum coefficient m was defined by:

$$m = \min(1 - 1 / (\text{current_iter} + 1), m_0), \quad (18)$$

where current_iter is the current iteration number of the training and $m_0 = 0.97$ is the upper bound set for m . After the momentum coefficient m was obtained, the parameters of the empirical model were updated according to Equation (11).

The classification performance of each compared method on ImageNet is illustrated in Table 6. FreMatch achieved a top-1 error rate of 41.80% and a top-5 error rate of 19.20% on ImageNet when 10% labelled data were used.

TABLE 7

Training Cost Per Epoch for Different Methods on an NVIDIA GeForce RTX 1080

Method	Training Cost (Min)
FixMatch [15]	6.21
SimMatch [34]	5.40
Semi-Clustering [41]	7.23
FlexMatch [39]	5.55
NP-Match [50]	6.10
DoubleMatch [42]	6.31
FreMatch	6.29

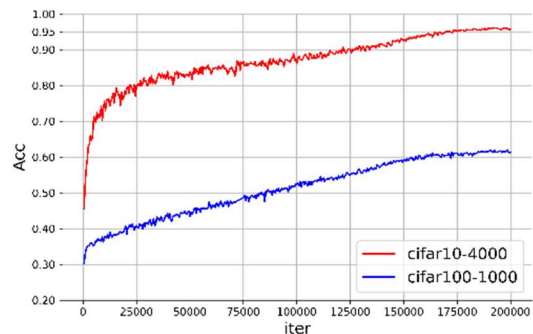


Fig. 3. Convergence of FreMatch for CIFAR-10 with 4000 labels and CIFAR-100 with 1000 labels

4.4 Computational Costs of Training

Table 7 shows the average training cost of each epoch for the method with each model structure on Cifar10 with 4000 labels. The training costs of FreMatch and DoubleMatch are very close because they employ a similar model structure, namely, the Siamese network structure.

The training cost of FixMatch is only slightly smaller than that of FreMatch, indicating that employing the momentum-based method to update the empirical model and using feature space renormalization had no significant effect on the computational cost of the training process. In SimMatch, the weakly augmented unlabelled samples are fed to the exponential moving average (EMA) model. Since the EMA does not need to perform back propagation, SimMatch had the lowest training cost among all the compared methods. In Semi-Clustering, the training process needs to alternate between SSL and deep clustering learning, so it takes longer to train.

We show in Fig. 3 the convergence of the classification accuracies over the training iterations of FreMatch for CIFAR-10 with 4000 labels and CIFAR-100 with 1000 labels. For CIFAR-100 with 1000 labels, although the number of categories in the dataset was larger and the amount of labelled data was smaller, the convergence of the training process for FreMatch was still stable, without drastic fluctuation. As seen from the figure, after training for 400 epochs, that is, 200,000 iterations, the accuracy converged to a relatively stable value in both cases.

4.5 Ablation Study

Since FreMatch combines two techniques, i.e., feature space renormalization and pseudo-labelling, we performed ablation studies to gain deeper insight into why it can obtain overall better results. Due to space limitations, in this subsection, we present only the results for experiments with 250 labels and 4000 labels in CIFAR-10.

4.5.1 Feature Space Renormalization and Pseudo-labelling

This subsection investigates how feature space renormalization and pseudo-labelling influence the performance of FreMatch. The experiments were conducted on CIFAR-10, and only the results for the experiments with 25 and 400 labels per class were recorded. As shown in Table 8, the error rates of FreMatch_F (i.e., FreMatch with only feature space renormalization) are

higher than those of FreMatch_P (i.e., FreMatch with only pseudo-labelling), but the combination of these two strategies resulted in the better performance of FreMatch than FreMatch_F and FreMatch_P.

In FreMatch_F, the features are utilized before the classification layer for feature space renormalization, and the classification layers of the basic model and the empirical model only learn from labelled samples. However, in FreMatch_P, the models learn from both labelled samples and unlabelled samples. It is thus understandable why FreMatch_F has a higher probability of yielding a higher error rate than does FreMatch_P.

We compared the performance of FreMatch_F with different dimensions of the features, and the results are illustrated in Table 9. FreMatch_128 denotes FreMatch_F using the 128 dimensions of features before the classification layer, and FreMatch_10 denotes FreMatch_F using the 10 dimensions of features before the softmax function. Owing to the poor performance, we do not list the results for FreMatch_10 with 250 labels. It is clear from the table that the error rate of FreMatch_10 is much higher than that of FreMatch_128.

According to the results shown in Table 8, pseudo-labelling in FreMatch makes two contributions to the model performance. The first is that it allows the classification layer to learn the category information from unlabelled samples, specifically the mapping from the feature representation to the corresponding category. The second is that it implements entropy minimization. In FreMatch, the sequential combination of feature space renormalization and pseudo-labelling is not just a simple hybrid of the two mechanisms but causes them to enhance each other. That is, feature space renormalization can provide a better feature representation for pseudo-labelling, and pseudo-labelling in turn can improve the ability of category discrimination, which feature space renormalization lacks. As a result, FreMatch can obtain overall good performance on the benchmark datasets.

TABLE 8

The Results of the Ablation Study on the Influence of Feature Space Renormalization and Pseudo-labelling on FreMatch

Model	Method		CIFAR-10	
	Feature Space Renormalization	Pseudo-Label	250 labels	4000 labels
FreMatch_F	✓	×	10.36±0.26	7.86±0.15
FreMatch_P	×	✓	6.08±0.23	4.07±0.14
FreMatch	✓	✓	4.95±0.34	3.47±0.21

TABLE 9

The Results of the Ablation Study for Different Dimensions of Features with Only Feature Space Renormalization

Model	Method (With only feature space renormalization)	CIFAR-10	
		250 labels	4000 labels
FreMatch_128	Use feature map $\psi \in \mathbb{R}^{n \times d}$ ($d = 128$)	10.36±0.26	7.86±0.15
FreMatch_10	Use feature map $\psi \in \mathbb{R}^{n \times d}$ ($d = 10$)	-	16.44±0.14

4.5.2 Feature Space Renormalization with Other SSL Methods

Feature space renormalization is an effective and general-

purpose feature regularization method that can be integrated with other SSL methods. Thus, this subsection aims to verify its effectiveness and generality for other SSL approaches.

First, we applied the widely used SSL framework FixMatch to verify that the feature space renormalization mechanism can be effective for training SSL with a Siamese network structure.

4.5.2.1 FixMatch with Feature Space Renormalization

First, we integrated the feature space renormalization mechanism into FixMatch to examine the generality of the proposed method. FixMatch obtains the loss of the unlabelled data by using both consistency regularization

and pseudolabelling on a single model. In contrast, we employed the Siamese network structure in the proposed FreMatch. In this work, FixMatch-Fre-Single and FixMatch-Fre-Siamese represent the integration of feature space renormalization with the single model and with the Siamese model, respectively, into FixMatch. In [15], λ was the weight of the unlabelled loss for FixMatch, and it was recommended to set it to 1.0. In the previous subsection, we set λ to 20.0 for FreMatch. Therefore, in this subsection, we set λ to 1.0 and 20.0 for both FixMatch-Fre-Single and FixMatch-Fre-Siamese in the experiments to investigate the influence of different λ values on the performance of the models.

TABLE 10
Error Rates of FixMatch with Feature Space Renormalization for CIFAR-10 on Two Different Numbers of Labelled Images

Model	CIFAR-10	
	250 labels	4000 labels
FixMatch [15]	5.07±0.65	4.26±0.05
FixMatch-Fre-Single (<i>unlabel</i> – weight $\lambda = 1.0$)	5.87±0.40	4.38±0.23
Fixmatch-Fre-Single (<i>unlabel</i> – weight $\lambda = 20.0$)	5.67±0.52	4.23±0.33
Fixmatch-Fre-Siamese (<i>unlabel</i> – weight $\lambda = 1.0$)	5.10±0.23	4.26±0.03
Fixmatch-Fre-Siamese (<i>unlabel</i> – weight $\lambda = 20.0$)	4.98±0.30	3.45±0.22

As shown in Table 10, FixMatch-Fre-Siamese had similar performance to the original FixMatch when λ was set to 1.0. Fixmatch-Fre-Single obtained poor classification performance, worse than that of the original Fixmatch, regardless of which value λ took. However, when FixMatch-Fre employed the Siamese network structure, i.e., the same model structure as the proposed FreMatch, Fixmatch-Fre-Siamese performed better than FixMatch if λ was set to a larger value.

According to the above, the Siamese network structure and the larger λ have a positive effect on feature space renormalization. In fact, a larger λ is desirable since it can exert a great penalty on ℓ_{fre} , as pointed out in Section 3. In addition, since MixMatch and ReMixMatch employ the mixing method to generate pseudo-labels, the proposed feature space renormalization mechanism is not suitable for integration with them.

4.5.2.2 Other SSL Methods with Feature Space Renormalization

According to the experiments for the benchmark datasets in subsection 4.1, FreMatch was not able to achieve better classification performance when using only a small number of labelled samples. Therefore, in this subsection, we couple feature space renormalization with the current methods that can achieve good classification performance with only a very small number of labelled samples. In this way, we can verify the generalization performance of feature space renormalization on the one hand, and on the other hand, we can determine which improvement strategy used in SSL can compensate for the insufficiency

of feature space renormalization in training the model with a very small number of labelled data.

Table 11 shows the classification performance of the SSL methods with and without feature space renormalization for the CIFAR-10 dataset. Overall, the feature space renormalization mechanism helped to improve the classification performance of these models. However, the performance of FlexMatch_Fre was lower than that of the original method.

TABLE 11
Error Rates of Other Methods with Feature Space Renormalization for CIFAR-10 on Two Different Numbers of Labelled Images

Methods	CIFAR-10	
	250 labels	4000 labels
Semi-Clustering	5.51	4.62
Semi-Clustering-Fre	4.63	3.77
FeatMatch	7.50	4.91
FeatMatch-Fre	7.04	4.40
FlexMatch	4.98	4.19
FlexMatch-Fre	5.58	4.20
SimMatch	4.84	3.96
SimMatch-Fre	4.55	3.20
NP-Match	4.96	4.11
NP-Match-Fre	4.23	4.05

When the number of labelled samples of each class is very small, the learning on unlabelled data in SSL completely depends on the pseudo-labels obtained in the supervised learning stage, so an increasing number of incorrect pseudo-labels can be generated but cannot be

corrected in subsequent learning. Therefore, many works focus on improving the quality of pseudo-labels. For example, Semi-Clustering is a combination of SSL with deep clustering, alternating between semi-supervised learning and clustering during the training process. SSL is implemented to stabilize and accelerate the training of the clustering stage. Through clustering the data, the centroids of the resultant clusters can provide the distribution information of unlabelled samples to the SSL phase to gradually improve the classification performance. This is equivalent to providing pseudo-labels implicitly in the clustering process so that the model is not prone to fitting a small number of data points when these data points do not agree well with the total data distribution. Therefore, Semi-Clustering can generate better pseudo-labels for the learning process on unlabelled data, effectively improving the performance of SSL as an overall result.

TABLE 12
Error Rates of FlexMatch_Fre with a truncation threshold for the CIFAR-10 and SVHN datasets

Methods	CIFAR-10		SVHN
	250 labels	250 labels	500 labels
FlexMatch	4.98	6.59	6.79
FlexMatch_Fre	4.10	3.54	3.18

The core of feature space renormalization is its employment of empirical features to guide the learning of the model. When there are more labelled data, we can obtain better feature representations that fit well with the data distribution. Therefore, the classification performance of the trained model can be generally better than that of the model trained without feature space renormalization.

However, when there are only a few labelled data, the process of empirical feature learning is disturbed by a continuously increasing number of incorrect pseudo-labels, which in turn can degrade the classification performance of FlexMatch. For the same reasons as for Semi-Clustering, SimMatch and NP-Match provide effective methods of improving the quality of pseudo-labels. Therefore, these strategies, combined with feature space renormalization, can effectively enhance the classification performance. FlexMatch_Fre essentially employs empirical features for feature-based augmentation, which can thus improve the classification performance. However, there is no strategy to improve the quality of pseudo-labels for FlexMatch_Fre, so its performance improvement is very limited when a small number of labelled data are used.

FlexMatch employs the curriculum pseudo-labelling (CPL) strategy, which aims to flexibly adjust the threshold for different classes in each training iteration so that FlexMatch can learn from more unlabelled data and their pseudo-labels. For FlexMatch, a lower threshold is used in the early stage of training to make full use of unlabelled data, but such a strategy may also create many incorrect labels among the pseudo-labels. This may be the main reason for the decreased performance of FlexMatch_Fre and the higher error rate of FlexMatch for the SVHN dataset. In contrast to FlexMatch, fixed and higher thresholds are used during the training process of FlexMatch_Fre. A fixed truncation threshold of 0.75 was used for FlexMatch_Fre. This means that unlabelled samples with prediction confidence lower than the truncation threshold are not used in the early stage of training. As shown in Table 12, FlexMatch_Fre with a truncation threshold of 0.75 had improved classification accuracies for both the CIFAR-10 and SVHN datasets.

TABLE 13
The Results of the Ablation Study on Different Optimizers with Different Learning Rates (lr) and Momenta (mom)

Optimizer	Hyperparameters	CIFAR-10	
		250 labels	4000 labels
SGD	$lr=0.01, mom=0.9$	4.95±0.34	3.47±0.21
SGD	$lr=0.01, mom=0$	6.13±0.10	3.52±0.11
SGD	$lr=0.01, mom=0.9, Nesterov$	5.05±0.34	3.47±0.44
SGD	$lr=0.025, mom=0.9$	5.22±0.03	3.59±0.03
SGD	$lr=0.005, mom=0.9, Nesterov$	5.15±0.13	3.54±0.13
Adam	$lr=0.01, wd=1e-3$	50.23±0.13	28.34±0.13

4.6 Optimizers and Learning Rate Schedule

We found that different optimizers and their hyperparameters also had an effect on the performance of the model. As shown in Table 13, SGD with a momentum of 0.9 generated better results, with the error rate for 250 labels reduced by 1.18% compared to that without momentum. It is also shown that the Nesterov variant of momentum did not yield an obvious improvement in the results. Moreover, we employed different initial learning rates but found no improvement in classification

performance. When Adam was used, relatively poor model performance was observed.

TABLE 14
The Results of the Ablation Study with Different Learning Rate Schedulers

Learning Rate Decay Scheduler	CIFAR-10	
	250 labels	4000 labels
Cosine ($min_lr=1e-4$)	4.95±0.34	3.47±0.21
Exp-Warmup ($min_lr=1e-4$)	5.23±0.03	4.09±0.22
No Decay	13.02±0.23	7.80±0.11

Regarding decay methods for the learning rate, it is a common choice in many recent works to employ a cosine scheduler [23]. For the purpose of performance verification, we compared this method with two other approaches, namely, Exp-warmup and the method without learning

rate decay. The classification error rates of the three decay methods are listed in Table 14. The results show that the cosine scheduler yielded the best classification results on the tested datasets.

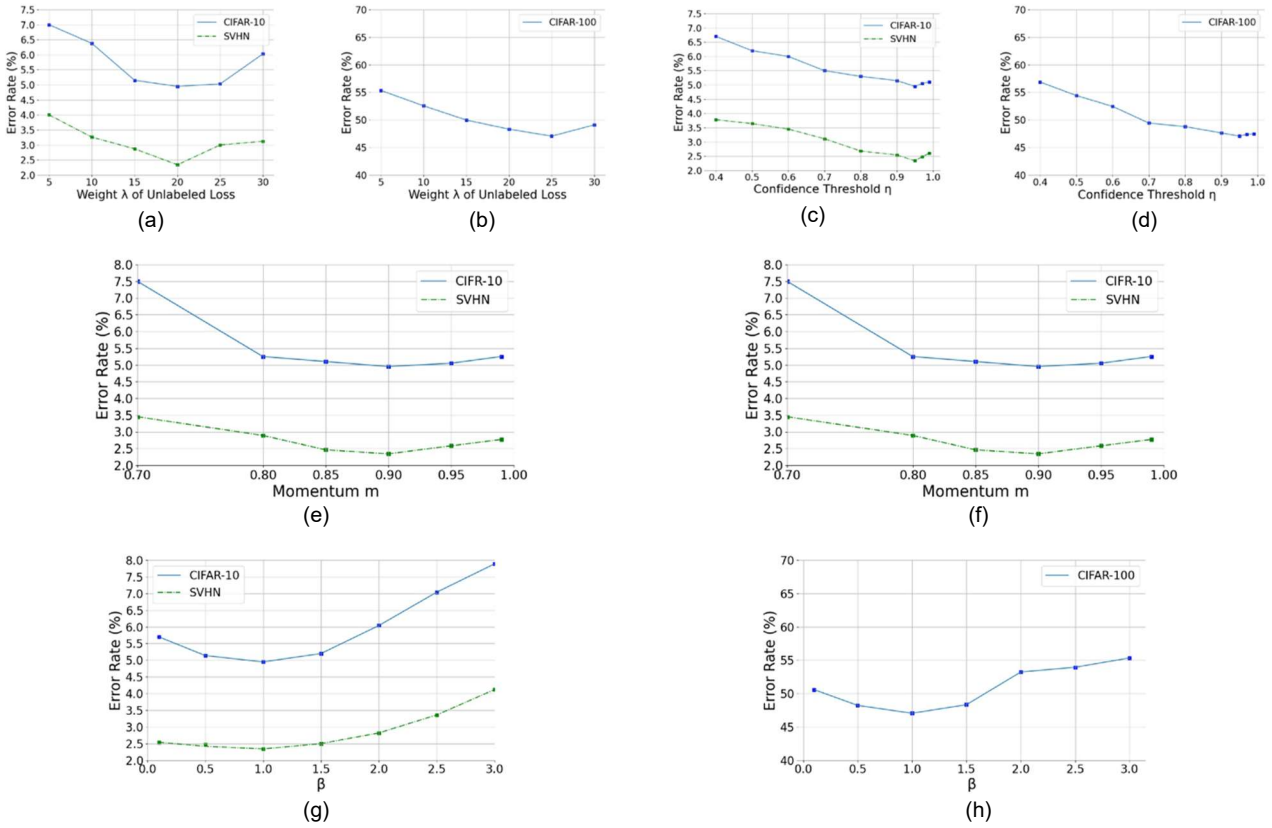


Fig. 4. The results of multiple hyperparameters on FreMatch are shown in the figures. We carried out experiments on CIFAR-10 and SVHN, both with 250 labelled images, and on CIFAR-100 with 400 labelled images. In (a) and (b), the error rates are shown for varying weights λ of unlabelled data loss. In (c) and (d), the error rates are shown for varying confidence thresholds η for pseudo-labelling. In (e) and (f), the error rates are shown for varying momentum coefficients m for updating the empirical model. In (g) and (h), the error rates are shown for varying scalar hyperparameters β for feature space renormalization.

4.7 Selection of Hyperparameters

FreMatch integrates feature space renormalization and pseudo-labelling to learn from unlabelled data, and it has four hyperparameters, namely, λ , η , m and β . To examine the performance sensitivity of the model to the value of each hyperparameter, we carried out experiments on CIFAR-10 and SVHN, both with 250 labelled images, and on CIFAR-100 with 400 labelled images. We tested the performance of FreMatch with a series of combinations of different values of the four hyperparameters. The results in Fig. 4 show that when $\eta = 0.95$ and $\beta = 1.0$, the model can yield the best result for each of the datasets. However, the values of λ and m that resulted in the best performance varied with different datasets. Due to space limitations, we only show in Fig. 4 the performance sensitivity of the model to the value of each hyperparameter for each benchmark dataset, with the remaining four hyperparameters fixed at their own optimal values.

With regard to λ , the weight of the unlabelled loss term, it is a common method to increase its value over the training process in SSL approaches [10, 11, 45]. However, in our work, λ is fixed at a large value, but a threshold for pseudo-labelling is set; the justification for this was given in subsection 3.6. The results for different values of λ , with the other hyperparameters fixed at their own optimal values, are shown in Fig. 4 (a) and (b). When $\lambda = 25$ for CIFAR-100 and $\lambda = 20$ for the other two benchmark datasets, the model was able to obtain the best performance for the corresponding dataset.

Fig. 4 (c) and (d) show the error rates of classification obtained by FreMatch on the three benchmark datasets for different values of η with the other hyperparameters fixed at their own optimal values. It is apparent that when $\eta = 0.95$, the best performance can be obtained for all three datasets. When η becomes larger, no further performance improvement can be achieved. However, when η is lower than 0.9, the performance of the model deteriorates significantly.

Fig. 4 (e) and (f) illustrate how the value of m influences the model performance for the three datasets with the other three hyperparameters fixed at their own optimal values. When $m = 0.97$ for CIFAR-100 and $m = 0.9$ for the other two benchmark datasets, the model was able to obtain the best performance on the corresponding datasets.

In Fig. 4 (g) and (h), the classification error rates of the model with different settings of β for each of the three datasets are shown. The results reveal that $\beta = 1.0$ can result in the best performance on each of the benchmark datasets.

5 CONCLUSIONS AND FUTURE WORK

Although SSL has made rapid progress recently, unfortunately, most of the advancement has been made at the cost of increasingly complicated learning algorithms with sophisticated data perturbation methods used in consistency regularization or pseudo-labelling. In this paper, we proposed FreMatch, a new SSL algorithm that obtained better performance on a variety of standard SSL benchmark datasets. The feature space renormalization mechanism, the main contribution of this work, when combined with pseudo-labelling, can improve the discrimination ability of FreMatch. We also show that when feature space renormalization was incorporated into other state-of-the-art SSL approaches, it can also help to enhance the performance of these approaches. This means that the feature renormalization mechanism, as a generic approach to renormalizing features in the feature space, can yield better discrimination of the models than regularizing consistency at the decision level.

Although FreMatch was not able to obtain the best results for some cases in the experiments, we are convinced by the experimental results that feature space renormalization is a promising and general-purpose method that provides a new direction for feature representation learning. Therefore, in the future, we will incorporate the feature space renormalization mechanism with other models to explore new possibilities.

REFERENCES

- [1] J. Deng, W. Dong, R. Socher, L. Li, Kai Li and Li Fei-Fei, "ImageNet: A large-scale hierarchical image database," *Proc. IEEE Conf. Comput. Vis. and Pattern Recognit.*, pp. 248-255, 2009.
- [2] T.-Y. Lin, M. Maire, S. Belongie, J. Hays, P. Perona, D. Ramanan, et al., "Microsoft coco: Common objects in context." *Proc. Eur. Conf. Comput. Vis.*, pp. 740-755, Sep. 2014.
- [3] Q. Xie, M. T. Luong, E. Hovy et al., "Self-training with noisy student improves imagenet classification." in *Proc. IEEE/CVF Conf. Comput. Vis. Pattern Recognit.*, pp. 10687-10698.
- [4] D. Mahajan, R. Girshick, V. Ramanathan, K. He, M. Paluri, Y. Li, et al., "Exploring the limits of weakly supervised pretraining." *Proc. Eur. Conf. Comput. Vis. (ECCV)*, pp. 181-196.
- [5] J. Hestness, S. Narang, N. Ardalani, G. Diamos, H. Jun, H. Kianinejad, et al., "Deep learning scaling is predictable, empirically." *arXiv preprint arXiv:1712.00409*.
- [6] B. H. Menze, A. Jakab, S. Bauer, J. Kalpathy-Cramer, K. Farahani, J. Kirby, et al., "The multimodal brain tumor image segmentation benchmark (BRATS)." *IEEE Trans. Med. Imaging*, vol. 34, no. 10, pp. 1993-2024, Oct. 2015.
- [7] O. Chapelle, B. Scholkopf, A. Zien, "Semi-supervised learning" *IEEE Trans. Neural Networks*, vol. 20, no. 3, pp. 542-542, 2006.
- [8] S. Laine, T. Aila. "Temporal ensembling for semi-supervised learning." *arXiv preprint arXiv:1610.02242*, 2016.
- [9] A. Tarvainen, H. Valpola. "Mean teachers are better role models: Weight-averaged consistency targets improve semi-supervised deep learning results." *Advances Neural Inf. Process. Syst.*, vol. 30, 2017.
- [10] D. Berthelot, N. Carlini, I. Goodfellow, N. Papernot, A. Oliver, C. Raffel. "Mixmatch: A holistic approach to semi-supervised learning." *Advances Neural Inf. Process. Syst.*, vol. 32, 2019.
- [11] D. Berthelot, N. Carlini, E. D. Cubuk, A. Kurakin, K. Sohn, H. Zhang, C. Raffel. "Remixmatch: Semi-supervised learning with distribution alignment and augmentation anchoring." *arXiv preprint arXiv:1911.09785*, 2019.
- [12] D. H. Lee, D. H. "Pseudo-label: The simple and efficient semi-supervised learning method for deep neural networks." In *Workshop on challenges in representation learning, ICML*, vol. 3, no. 2, p. 896, June. 2013.
- [13] P. Bachman, O. Alsharif, D. Precup. "Learning with pseudo-ensembles." *Advances Neural Inf. Process. Syst.*, vol. 27, pp. 3365-3373, 2014.
- [14] Q. Xie, Z. Dai, E. Hovy, M. Y. Luong, Q. V. Le. "Unsupervised data augmentation for consistency training." *Advances Neural Inf. Process. Syst.*, vol. 33, pp. 6256-6268, 2019.
- [15] K. Sohn, D. Berthelot, C. L. Li, Z. Zhang, N. Carlini, E. D. Cubuk, C. Raffel, "Fixmatch: Simplifying semi-supervised learning with consistency and confidence." *Advances Neural Inf. Process. Syst.*, vol. 33, pp. 596-608, 2020.
- [16] T. DeVries, G. W. Taylor. "Improved regularization of convolutional neural networks with cutout." *arXiv preprint arXiv:1708.04552*, 2017.
- [17] S. Lim, I. Kim, T. Kim, C. Kim, S. Kim, "Fast autoaugment." *Advances Neural Inf. Process. Syst.*, vol. 32, pp. 6665-6675, 2019.
- [18] A. Gammnerman, V. Vovk, V. Vapnik. "Learning by transduction." *arXiv preprint arXiv:1301.7375*, 2013.
- [19] T. Joachims. "Transductive learning via spectral graph partitioning." *Proc. Int. Conf. Mach. Learn. (ICML)*, pp. 290-297, 2003.
- [20] X. Zhu, Z. Ghahramani, J. D. Lafferty, "Semi-supervised learning using gaussian fields and harmonic functions." *Proc. Int. Conf. Mach. Learn. (ICML)*, pp. 912-919, 2003.
- [21] Y. Bengio, O. Delalleau, N. Le Roux, "Label Propagation and Quadratic Criterion." ch. 11, MIT Press, 2006.
- [22] B. Liu, Z. Wu, H. Hu, S. Lin, "Deep metric transfer for label propagation with limited annotated data." *Proc. Int. Conf. Comput. Vis. Workshop*, pp. 0-0, 2019.
- [23] A. Coates, A. Y. Ng, "The importance of encoding versus training with sparse coding and vector quantization." *Proc. Int. Conf. Mach. Learn. (ICML)*, pp. 921-928, Jan. 2011.
- [24] D. P. Kingma, S. Mohamed, D. J. Rezende, M. Welling, "Semi-supervised learning with deep generative models." *Advances Neural Inf. Process. Syst.*, pp. 3581-3589, 2014.
- [25] A. Odena, "Semi-supervised learning with generative adversarial networks." *arXiv preprint arXiv:1606.01583*, 2016.
- [26] T. Miyato, A. M. Dai, I. Goodfellow, "Adversarial training

- methods for semi-supervised text classification." *arXiv preprint arXiv:1605.07725*, 2016.
- [27] J. E. Van Engelen, H. H. Hoos, "A survey on semi-supervised learning." *Mach. Learn.*, vol. 109, no. 2, pp. 373-440, 2020.
- [28] M. Tuchler, A. C. Singer, R. Koetter, "Minimum mean squared error equalization using a priori information." *IEEE Trans. Signal Process.*, vol. 50, no. 3, pp. 673-683, 2002.
- [29] J. Goldberger, S. Gordon, H. Greenspan, "An Efficient Image Similarity Measure Based on Approximations of KL-Divergence Between Two Gaussian Mixtures." *Proc. Int. Conf. Comput. Vis.*, Vol. 3, pp. 487-493, Oct. 2003.
- [30] J. R. Hershey, P. A. Olsen, "Approximating the Kullback Leibler divergence between Gaussian mixture models." *IEEE Int. Conf. Acoust. Speech Signal Process. (ICASSP)*, vol. 4, pp. IV-317, April. 2007.
- [31] P. T. De Boer, D. P. Kroese, S. Mannor, R. Y. Rubinstein, "A tutorial on the cross-entropy method." *Ann. Operations Res.*, vol. 134, no. 1, pp. 19-67, 2005.
- [32] M. Sajjadi, M. Javanmardi, T. Tasdizen, "Regularization with stochastic transformations and perturbations for deep semi-supervised learning." *Advances Neural Inf. Process. Syst.*, vol. 29, pp. 1163-1171, 2016.
- [33] E. D. Cubuk, B. Zoph, D. Mane, V. Vasudevan, Q. V. Le, "Autoaugment: Learning augmentation policies from data." *arXiv preprint arXiv:1805.09501*, 2018.
- [34] M. Zheng, S. You, L. Huang, F. Wang, C. Qian, & C. Xu, "Simmatch: Semi-supervised learning with similarity matching.", *Proc. IEEE Conf. Comput. Vis. and Pattern Recognit*, pp. 14471-14481, 2022.
- [35] G. J. McLachlan, "Iterative reclassification procedure for constructing an asymptotically optimal rule of allocation in discriminant analysis." *J. Amer. Statistical Assoc.*, vol. 70, no. 350, pp. 365-369, 1975.
- [36] H. Scudder, "Probability of error of some adaptive pattern-recognition machines." *IEEE Trans. Inf. Theory*, vol. 11, no. 3, pp. 363-371, 1965.
- [37] Y. Grandvalet, Y. Bengio, "Semi-supervised learning by entropy minimization." *Advances Neural Inf. Process. Syst.*, vol. 365, pp. 281-296, 2005.
- [38] M. Sajjadi, M. Javanmardi, T. Tasdizen, "Mutual exclusivity loss for semi-supervised deep learning." *IEEE Int. Conf. Image Process. (ICIP)*, pp. 1908-1912, Sep. 2016.
- [39] B. Zhang, Y. Wang, W. Hou, H. W. J. Wang, M. Okumura, & T. Shinozaki. "Flexmatch: Boosting semi-supervised learning with curriculum pseudo labeling." *Advances Neural Inf. Process. Syst.*, vol. 34, 2021.
- [40] C. W. Kuo, C. Y. Ma, J. B. Huang, & Z. Kira, "Featmatch: Feature-based augmentation for semi-supervised learning.", *Proc. Eur. Conf. Comput. Vis. (ECCV)*, pp. 479-495, Aug, 2020.
- [41] B. Lerner, G. Shiran, & D. Weinshall, "Boosting the performance of semi-supervised learning with unsupervised clustering.", *arXiv preprint arXiv:2012.00504*, 2022.
- [42] E. Wallin, L. Svensson, F. Kahl, & L. Hammarstrand, "DoubleMatch: Improving Semi-Supervised Learning with Self-Supervision.", *Proc. Int. Conf. Comput. Vis. (ICPR)*, pp. 2871-2877, Aug, 2022.
- [43] A. Baker, "Matrix groups: an introduction to Lie group theory", *Springer Science & Business Media*, 2002.
- [44] J. Brazas, "The fundamental group as a topological group." *Topology and its Appl.*, vol. 160, no. 1, pp. 170-188, 2013.
- [45] B. Steinberg, "Representation theory of finite groups: an introductory approach.", *Springer*, 2012.
- [46] A. Krizhevsky, G. Hinton, "Learning multiple layers of features from tiny images." *Handbook of Systemic Autoimmune Diseases*, 2009.
- [47] Y. Netzer, T. Wang, A. Coates, A. Bissacco, B. Wu, A. Y. Ng, "Reading digits in natural images with unsupervised feature learning.", In *NIPS Workshop Deep Learn. Unsupervised Feature Learn.*, 2011.
- [48] A. Oliver, A. Odena, C. Raffel, E. D. Cubuk, I. J. Goodfellow, "Realistic evaluation of deep semi-supervised learning algorithms." *Advances Neural Inf. Process. Syst.*, vol. 31, 2018.
- [49] A. Rasmus, H. Valpola, M. Honkala, M. Berglund, T. Raiko, "Semi-supervised learning with ladder networks." *Advances Neural Inf. Process. Syst.*, vol. 28, 2015.
- [50] A. Coates, A. Ng, H. Lee, "An analysis of single-layer networks in unsupervised feature learning." *Proc. Int. Conf. Artif. Intell. Statist.*, pp. 215-223, June. 2011.
- [51] E. D. Cubuk, B. Zoph, J. Shlens, & Q. V. Le, Q. V., "Randaugment: Practical automated data augmentation with a reduced search space." *Proc. IEEE Conf. Comput. Vis. and Pattern Recognit*, pp. 702-703, 2020.
- [52] S. Zagoruyko, & N. Komodakis, "Wide residual networks.", *arXiv preprint arXiv:1605.07146*, 2016.
- [53] H. Pham, Z. Dai, Q. Xie, & Q. V. Le, "Meta pseudo labels.", *Proc. IEEE Conf. Comput. Vis. and Pattern Recognit*, pp. 11557-11568, 2021.
- [54] J. Wang, T. Lukasiewicz, D. Masiceti, X. Hu, V. Pavlovic, & A. Neophytou, "Np-match: When neural processes meet semi-supervised learning.", *Proc. Int. Conf. Mach. Learn. (ICML)*, pp. 22919-22934, June, 2022.
- [55] K. Saenko, B. Kulis, M. Fritz, & T. Darrell, "Adapting visual category models to new domains." *Proc. Eur. Conf. Comput. Vis. (ECCV)*, pp. 213-226, September, 2010.
- [56] H. Venkateswara, J. Eusebio, S. Chakraborty, & S. Panchanathan, "Deep hashing network for unsupervised domain adaptation." *Proc. IEEE Conf. Comput. Vis. and Pattern Recognit*, pp. 5018-5027, 2017.
- [57] X. Peng, Q. Bai, X. Xia, Z. Huang, K. Saenko, & B. Wang, "Moment matching for multi-source domain adaptation." *Proc. Int. Conf. Comput. Vis.*, pp. 1406-1415, 2019.
- [58] K. He, X. Zhang, S. Ren, & J. Sun, "Deep residual learning for image recognition.", *Proc. IEEE Conf. Comput. Vis. and Pattern Recognit.*, pp. 770-778, 2016.



Jun Sun received his PhD in control theory and engineering, and an MSc in Computer Science and Technology from Jiangnan University, China, in 2009 and 2003, respectively. He is currently working as a full Professor with the Department of Computer Science and Technology, Jiangnan University, China. He is also vice director of Jiangsu Provincial Engineering Laboratory of Pattern Recognition and Computational Intelligence, Jiangsu Province. His major research areas and work are related to computational intelligence, machine learning, bioinformatics, among others. He published more than 150 papers in journals, conference proceedings and several books in the above areas.



Zhongjie Mao studied for a master's degree in computer science and technology at the School of Internet of Things Engineering in Jiangnan University, China, in 2016. He is currently working toward the PhD degree in pattern recognition and intelligent systems in the Jiangsu Provincial Engineering Laboratory of Pattern Recognition and Computational Intelligence, Jiangnan University, Wuxi, China. His research interests include computer vision, semi-supervised learning and representation

learning.



Chao Li received his Bachelor Degree in Information Engineering from Nanjing University of Information Science and Technology, Nanjing, China, in 2012 and a Master Degree in Computer Science and Technology from Jiangnan University, Wuxi, China, in 2017. He is currently working as a PHD student in Control Science and Engineering in Jiangnan University, Wuxi, China. His research areas are related to computational intelligence, computer vision and

bioinformatics. He has published several papers in journals and conferences in the above areas.



Chao Zhou studied for a master's degree in computer science and technology at the School of Artificial Intelligence and Computer Science in Jiangnan University, China, in 2020. He is currently working toward the PhD degree in software engineering in the Jiangsu Provincial Engineering Laboratory of Pattern Recognition and Computational Intelligence, Jiangnan University, Wuxi, China. His research interests

include computer vision, representation learning and incremental learning.



Xiao-Jun Wu received his B.Sc. degree in mathematics from Nanjing Normal University, Nanjing, China, in 1991. He received the M.S. degree in 1996, and the Ph.D. degree in pattern recognition and intelligent systems in 2002, both from Nanjing University of Science and Technology, Nanjing, China. He joined Jiangnan University in 2006, where he is currently a Professor. He has published more than 200 papers in his fields of research. He

was a visiting researcher in the Centre for Vision, Speech, and Signal Processing (CVSSP), University of Surrey, U.K., from 2003 to 2004. His current research interests include pattern recognition, computer vision, fuzzy systems, neural networks, and intelligent systems.